frontiers in Chemistry

ORIGINAL RESEARCH
published: 16 April 2021
doi: 10.3389/fchem.2020.605311

Formaldehyde Molecules Adsorption on Zn Doped Monolayer MoS_2: A First-Principles Calculation

Huili Li[1†], Ling Fu[2,3†], Chaozheng He[4,5], Jinrong Huo[4], Houyong Yang[4,5], Tingyue Xie[6], Guozheng Zhao[1*] and Guohui Dong[7*]*

[1]Key Laboratory of Magnetic Molecules, Magnetic Information Materials Ministry of Education, The School of Chemistry and Material Science, Shanxi Normal University, Linfen, China, [2]College of Agricultural Engineering, Nanyang Normal University, Nanyang, China, [3]College of Resources and Environmental Engineering, Tianshui Normal University, Tianshui, China, [4]Institute of Environmental and Energy Catalysis, School of Materials Science and Chemical Engineering, Xi'an Technological University, Xi'an, China, [5]Shaanxi Key Laboratory of Optoelectronic Functional Materials and Devices, School of Materials Science and Chemical Engineering, Xi'an Technological University, Xi'an, China, [6]School of Physics and Electronic Science, Shanxi Datong University, Shanxi, China, [7]School of Environmental Science and Engineering, Shaanxi University of Science and Technology, Xi'an, China

OPEN ACCESS

Edited by:
Jinfeng Dong,
Wuhan University, China

Reviewed by:
Zhihua Xu,
Jianghan University, China
Xing Ding,
Huazhong Agricultural University, China

***Correspondence:**
Chaozheng He
hecz2019@xatu.edu.cn
Guozheng Zhao
zhaoguozheng@sxnu.edu.cn
Guohui Dong
dongguohui@sust.edu.cn

†These authors have contributed equally to this work

Specialty section:
This article was submitted to Catalysis and Photocatalysis, a section of the journal Frontiers in Chemistry

Received: 11 September 2020
Accepted: 17 December 2020
Published: 16 April 2021

Citation:
Li H, Fu L, He C, Huo J, Yang H, Xie T, Zhao G and Dong G (2021) Formaldehyde Molecules Adsorption on Zn Doped Monolayer MoS_2: A First-Principles Calculation. Front. Chem. 8:605311. doi: 10.3389/fchem.2020.605311

Based on the first principles of density functional theory, the adsorption behavior of H_2CO on original monolayer MoS_2 and Zn doped monolayer MoS_2 was studied. The results show that the adsorption of H_2CO on the original monolayer MoS_2 is very weak, and the electronic structure of the substrate changes little after adsorption. A new kind of surface single cluster catalyst was formed after Zn doped monolayer MoS_2, where the $ZnMo_3$ small clusters made the surface have high selectivity. The adsorption behavior of H_2CO on Zn doped monolayer MoS_2 can be divided into two situations. When the H-end of H_2CO molecule in the adsorption structure is downward, the adsorption energy is only 0.11 and 0.15 eV and the electronic structure of adsorbed substrate changes smaller. When the O-end of H_2CO molecule is downward, the interaction between H_2CO and the doped MoS_2 is strong leading to the chemical adsorption with the adsorption energy of 0.80 and 0.98 eV. For the O-end-down structure, the adsorption obviously introduces new impurity states into the band gap or results in the redistribution of the original impurity states. All of these may lead to the change of the chemical properties of the doped MoS_2 monolayer, which can be used to detect the adsorbed H_2CO molecules. The results show that the introduction of appropriate dopant may be a feasible method to improve the performance of MoS_2 gas sensor.

Keywords: first-principles calculation, monolayer MoS_2, H_2CO, adsorption energy, gas sensitivity

INTRODUCTION

In recent years, two-dimensional (2D) materials have attracted much attention due to their unique physical, chemical and electrical properties (Abbasi and Sardroodi, 2018a; Abbasi and Sardroodi, 2018b; Wu et al., 2018; Abbasi, 2019; Abbasi and Sardroodi, 2019). Among them, monolayer MoS_2 belongs to hexagonal system, which is a typical 2D layered transition metal sulfide with sheet structure similar to graphene (Pan et al., 2020). It has been studied due to the excellent electronic structure, chemical and thermal stability, high surface activity and high strength (Xu et al., 2013). Compared with the zero gap of graphene, single-layer MoS_2 has considerable direct band gap, which is suitable for light emitter, energy conversion and solar cell (Yu et al., 2016). Meanwhile, MoS_2 has

large specific surface area, surface activity and excellent adsorption capacity, so it is a special gas storage material or gas sensing material source (Zhang et al., 2017; Zhang et al., 2018; Zhou et al., 2018; Chen et al., 2019; Kathiravan et al., 2019; Tan et al., 2020). These excellent properties make the monolayer MoS_2 have potential applications in the field of gas sensing.

However, due to the lack of free bonds on the surface of intact MoS_2, which is chemically inert (Wang et al., 2013), the interaction with most gas molecules is limited to physical adsorption (Wanno and Tabtimsai, 2014), resulting in weak interaction between the adsorbent and monolayer MoS_2, and the change of electronic properties is not obvious, and the original MoS_2 cannot detect H_2CO gas molecule (Ma et al., 2016a). Therefore, it is an effective and feasible method to adjust the electronic structure, chemical activity and sensitivity of MoS_2 by introducing appropriate dopants into defect sites (Ma et al., 2016c; Sharma et al., 2018; Cui et al., 2019; Guo et al., 2019; Ren et al., 2019; Zhang et al., 2019; Guo et al., 2020; Zheng et al., 2020). For example, Lolla et al. have shown that Fe and Co. doped monolayer MoS_2 can enhance the adsorption of O due to the partial occupation of *d*-orbitals on Fermi level, and the introduction of doping significantly improves the catalytic activity of MoS_2 monolayer (Lolla and Luo, 2020). (Abbas et al., 2018) proposed that compared with the original monolayer MoS_2, N and P doped atoms can enhance the sensing sensitivity of monolayer MoS_2 to O_2 and NO gas molecules (Abbas et al., 2018). (Sahoo et al., 2016) have shown that the original monolayer MoS_2 is inert to gas molecules such as NH_3 and NO_2, and the detection sensitivity of antisite doped with MoS_2 for these gas molecules and other chemical substances is significantly improved (Sahoo et al., 2016). Luo et al. have shown that Al, Si and P doped atoms increase the orbital hybridization effect between NO_2, NH_3 molecules and monolayer MoS_2, and promote the electron transfer. The doped monolayer MoS_2 has better adsorption performance than the undoped monolayer MoS_2 (Luo et al., 2016). Ma et al. have shown that when Au, Fe, CO and Ni are doped into the monolayer MoS_2, the charge transfer occurs, the distance between the adsorbed molecule and the dopant is shortened, the adsorption energy is increased, and the gas sensitivity to H_2, CO, NO and O_2 is increased (Ma et al., 2016b; Kwak et al., 2018; Kwon et al., 2018; Wang et al., 2019a). Au doped monolayer MoS_2 has high charge transfer and strong orbital hybridization ability. Doping Au atoms affect the electronic structure of MoS_2 monolayer, thus improving the adsorption capacity, so that the adsorption structure of C_2H_6 and C_2H_4 molecules on Au doped MoS_2 monolayer is relatively stable (Qian et al., 2020). In conclusion, although there are some reports on the surface activity of doped monolayer MoS_2, the adsorption of formaldehyde on the surface of transition metal Zn doped MoS_2 has not been confirmed. Therefore, the geometry, electronic structure and small molecule adsorption of different transition metal atom doped monolayer MoS_2 system can be obtained by theoretical simulation method, which has guiding significance for the study of the unique gas sensing properties, adsorption properties and chemical activities of transition metal atom doped monolayer MoS_2.

At present, toxic gas molecules are one of the main problems of environmental pollution. H_2CO is a common toxic gas. H_2CO is widely used in household materials (Chung et al., 2013; Salthammer, 2013). Long term exposure to H_2CO will irritate the eyes and throat, make breathing difficult, and even pose a serious threat to the lungs. Therefore, it is of great significance to detect and control H_2CO in home, residence and scientific research (Lara-Ibeas et al., 2020; Song et al., 2020; Zhou et al., 2020). Based on the first principle calculation, this paper studies the changes of the configuration, geometric stability and electronic structure of MoS_2 substrate caused by the adsorption of H_2CO on the original and Zn doped monolayer MoS_2 gas after the S vacancy is filled with Zn dopant, and the adsorption energy, adsorption structure and charge transfer of gas molecules are analyzed. This study is helpful to find suitable chemical modification methods to improve the performance of MoS_2 based gas sensors, and has important scientific significance and application prospects for the design of high-efficiency gas sensing materials.

COMPUTING METHOD

All calculations were carried out using the first principle method, which was carried out by Vienna *Ab-initio* Simulation Package (VASP) and projector enhanced wave (PAW) method of DFT (Qian et al., 2019; Wang et al., 2019b). The configuration of transition metal Zn doped MoS_2 monolayer was optimized. The generalized gradient approximation (GGA) and perdew-Burke-Ernzerhof (PBE) are used to calculate the exchange correlation energy. The C *2s2p*, Zn *3d4s* and O *2s2p* states are regarded as valence electrons. In the process of geometric optimization, all internal coordinates are allowed to relax under a fixed lattice constant, and the energy cutoff for plane waves is set to 450 eV. The Brillouin domain integral uses $3 \times 3 \times 1$ (Monkhorst and Pack, 1976) monkhorst pack (MP) grid and 0.1 eV Gaussian smear. The convergence criterion is 10^{-5} eV. When the force applied to the atom is less than 0.01 ev/Å, the optimized structure is obtained. The calculated lattice constant of MoS_2 is 3.18 Å, which is well consistent with the experimental and theoretical value of 3.20 and 3.18 Å (Ataca and Ciraci, 2011; Le et al., 2014). Dispersive interactions are not included because we are concerned about the effects of chemical bonds and gas molecules on the electronic and magnetic properties of MoS_2. This method has been used to study gas adsorption on atom doped MoS_2 (Ma et al., 2016a). MoS_2 cell is constructed as a 4×4 supercell, in which one S atom is replaced by a Zn doped atom, with a total of 48 atoms, including 16 Mo atoms, 31 S atoms and one Zn atom. In order to avoid the interaction between the MoS_2 monolayer and its periodic image, a vacuum space of 18 Å was added perpendicular to the MoS_2 layer. The binding energy (E_b) between metal atom and support is defined as $E_b = E_{tot}$ (MoS_2-S) + E_{tot}(M) − E_{tot} (M + MoS_2), where E_{tot} (M + MoS_2), E_{tot} (MoS_2-S) and E_{tot} (M) are the total energy of M/MoS_2 catalyst, energy of MoS_2 vacancy S-based carrier and the energy of single metal atom, respectively. Positive values indicate that the reaction gives off heat. In addition, the adsorption energy (E_{ads}) was calculated to describe the interaction strength between gas and gas/MoS_2 catalyst. According to the formula $E_{ads} = E_{tot}$ (M + MoS_2) + E_{tot} (gas) − E_{tot} (gas-M/MoS_2), E_{tot} (M + MoS_2), E_{tot} (gas) and E_{tot} (gas-M/MoS_2) are the energy of M/MoS_2 catalyst, the energy of

gas and the total energy of adsorption system respectively. According to this definition, positive adsorption energy represents exothermic adsorption. The density of states (DOS) is calculated by using the *K* point 5 × 5 × 1 with higher density. The results of DOS were analyzed by P4vasp. Bader charge (Henkelman et al., 2006) was used to analyze the charge transfer. The 3D visualization program Vesta (Momma and Izumi, 2011) was used to visualize all molecular structures, and the electron density difference was obtained to analyze the electron transfer direction. The electron density difference is defined as $\triangle\rho = \rho_{gas\text{-}M/MoS2} - \rho_{M/MoS2} - \rho_{gas}$, where $\rho_{gas\text{-}M/MoS2}$, $\rho_{M/MoS2}$ and ρ_{gas} represent the electron density of adsorption system, M/MoS_2 catalyst and gas, respectively. The PAW results based on VASP processing and the COHP diagram of LOBSTER 4.0.0 (Local Orbital Basis Suite Towards Electronic-Structure Reconstruction) (Maintz et al., 2016) were used to analyze the bonding.

RESULTS AND DISCUSSION

Properties of Zn Doped Monolayer MoS_2 (Zn-MoS_2)

Seen from **Supplementary Figure S1A**, nine possible adsorption sites were considered for H_2CO adsorb on the original MoS_2 surface, where T_S, T_{Mo1}/T_{Mo2}, H_1/H_2 and $B_1/B_2/B_3$ represent the top of S and Mo atoms, hexagonal ring center and bridge sites. The T_{SV} represent the top site of Zn doped the S vacancy. As depicted in **Supplementary Figure S1B**, the band structure and total density of states (TDOS) of the original monolayer MoS_2 show that the original MoS_2 monolayer is a non-magnetic semiconductor with a direct band gap of 1.74 eV, which is well consistent with the results reported in the literature value of 1.74 eV (Dimple et al., 2017). The calculated binding energy of Zn doping on MoS_2 surface is 0.5 eV, which indicates that this structure is easy to form under thermodynamic equilibrium conditions due to the exothermic process. As shown in **Figure 1B**, the charge accumulation and loss can be observed in both Zn and Mo atoms, which means that chemical bonds are formed between Zn and Mo atoms in the $ZnMo_3$ clusters, which can be used as a new surface single cluster catalyst (SCC) (Ma et al., 2018) to study the adsorption performance of H_2CO molecules.

For the average bond length between Zn dopant and adjacent Mo atoms, the calculated average bond length of Zn-Mo is 2.65 Å, which is larger than that of S-Mo bond in original monolayer MoS_2 with the value of 2.41 Å. As exhibited in **Figure 1A**, accordingly the expansion of Zn-Mo bond relative to S-Mo bond makes the doped Zn atom protrude 0.26 Å above the S-plane. The electron transfer between dopant and MoS_2 is calculated by Bader charge analysis. The trend of charge transfer is consistent with that of element electronegativity (Allred, 1961). The paulin electronegativity of Mo is 2.16, which is greater than that of Zn (1.65). Accordingly, Zn dopant loses electrons and carries a positive charge of 0.35 *e*.

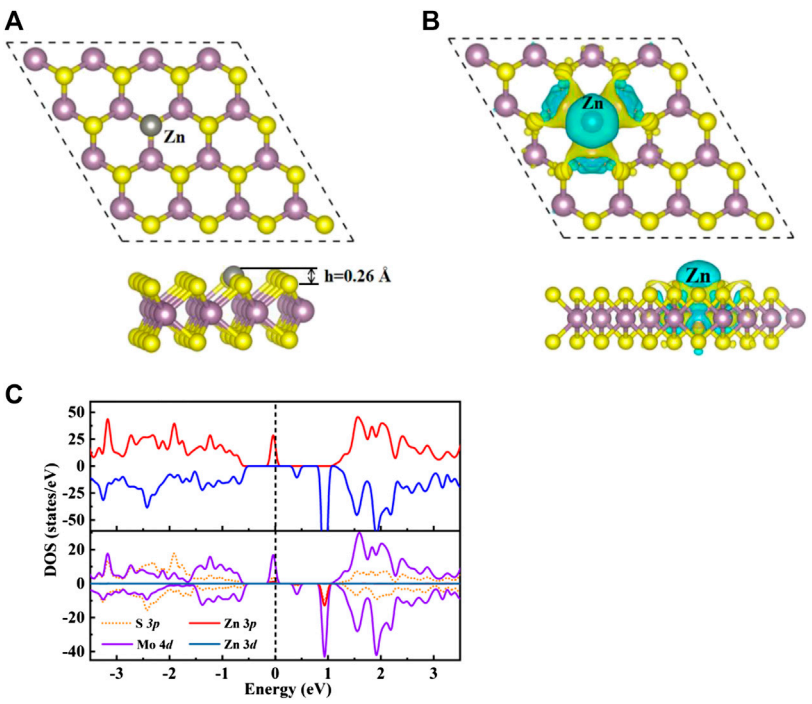

FIGURE 1 | (A) Optimize the top view **(top)** and side view **(bottom)** structure of Zn-MoS_2. Zn atoms are silver spheres. **(B)** The charge density difference diagram of Zn-MoS_2. The yellow area indicates charge accumulation and the cyan area indicates charge loss. **(C)** TDOS **(upper panels)** and PDOS **(lower panels)** of Zn-MoS_2 are projected on 3*p* orbital (red curve) and 3*d* orbital (dark blue curve) of Zn, 4*d* orbital (purple curve) of Mo atom and 3*p* orbit (orange dotted line) of S atom. The positive and negative values of DOS indicate spin up and spin down, respectively. The Fermi level is marked with a black dotted line.

TABLE 1 | Parameters of stable configuration of H_2CO adsorbed on original and Zn doped monolayer MoS_2: adsorption energy (E_{ad} in eV), charge obtained by H_2CO (Q_g in e), charge obtained by Zn (Q_{Zn} in e), magnetic moment of Zn atom (M_{Zn} in μ_B), nearest distance between adsorbed molecule and Zn atom ($d_{g\text{-}Zn}$ in Å), average distance between Zn atom and its adjacent molybdenum atom ($d_{s/Zn\text{-}Mo}$ in Å), The height of Zn atom relative to S plane (h in Å).

Configuration	E_{ad}	Q_g	Q_{Zn}	M	M_{Zn}	$d_{g\text{-}Zn}$	$D_{s/Zn\text{-}Mo}$	h
S/H_2CO	0.04	−0.01	0.00	0.00 (0.00)	0.00	3.13	2.41	0.00
Zn/H_2CO-(a)	0.98	−0.05	0.51	1.98 (0.05)	0.08	1.98	2.70	0.33
Zn/H_2CO-(B)	0.80	−0.09	0.53	1.97 (0.05)	0.08	1.95	2.70	0.28
Zn/H_2CO-(c)	0.15	0.07	0.33	2.00 (−0.01)	0.09	2.02	2.67	0.27
Zn/H_2CO-(d)	0.11	0.08	0.33	2.00 (−0.01)	0.10	2.02	2.66	0.25

For M (μ_B), the values inside and outside the brackets are the magnetic moment of the adsorbed molecule and the magnetic moment of the whole cell, respectively. It should be noted that S/H_2CO refers to the configuration shown in ***Figure 3A****, and the dopant of this configuration is actually S atom.*

The charge distribution of Zn-MoS_2 can be confirmed from **Figure 1B**. It is easy to see that Zn atoms are surrounded by cyan, which indicates that Zn atoms lose electrons. In addition, the magnetic moment of MoS_2 is produced by Zn doping, the total magnetic moment of the single-layer MoS_2 is 2.00 μ_B, only 0.1μ_B is located on the doped Zn atom, which indicates that the magnetic moment of the system mainly comes from Mo atom. In order to further understand the electronic and magnetic properties of Zn-MoS_2, the total DOS (TDOS) and projected DOS (PDOS) of Zn-MoS_2 spin polarization are given in **Figure 1C**. It can be seen from **Figure 1C** that an asymmetric DOS peak appears near the Fermi level, which is obviously different from the perfect MoS_2 monolayer. This is consistent with the fact that the Zn-MoS_2 system is paramagnetic (2.0 μb). Compared with MoS_2 monolayer **Supplementary Figure S1B**, the spin down channel of Zn-MoS_2 maintains the zero gap semiconductor characteristics of MoS_2, but the spin up channel presents a non-zero density of states near Fermi level which indicates that the Zn-MoS_2 system is semimetallic. Seen from the PDOS shown in **Figure 1C**, the degree of spin asymmetry of the 4*d* orbit of Mo is greater than that of the 3*d* orbit of Zn. This is consistent with the fact that the magnetic moment is mainly located on Mo atoms near Zn doping. In addition, since the asymmetric DOS peak is dominated by the 4*d* orbit of Mo, it can be expected that the spin charge density is mainly distributed on Mo atoms. Therefore, as shown in **Figure 1B**, the spin charge density of Zn-MoS_2 system is mainly concentrated around Mo atom. In addition, **Figure 1C** also shows that near the Fermi level, the 3*p* state of Zn atom is hybridized with the 4*d* orbital of Mo, indicating the interaction between metal atom and S-vacancy.

Adsorption of H_2CO on Original MoS_2 Monolayer

In order to obtain a stable configuration, various possible initial adsorption structures were considered **Supplementary Figure S1A**. The interaction between H_2CO and original MoS_2 is very weak, and the stable configuration obtained belongs to physical adsorption. In this work, only the configuration with the largest and most stable adsorption energy is discussed. The adsorption energy, charge transfer and other related parameters are shown in **Table 1**, and the geometric electronic structure is shown in **Figure 2**.

Seen from **Figure 2A**, the adsorption energy of H_2CO on the original monolayer MoS_2 is 0.04 eV. The adsorption of H_2CO is almost perpendicular to the plane, and the H-end is downward. The nearest distance between the molecule and the substrate is 3.13 Å. Due to the small adsorption energy, the interaction between the adsorbed molecules and the substrate is weak, and the geometric structure of the adsorbed molecules is almost undisturbed. The C-O bond length is about 1.21 Å, and C-H bond length is about 1.12 Å, which is the same as that of H_2CO bond in gas phase **Figure 2A**. The position of S atom under the adsorbed H_2CO does not change, and the bond length between S and Mo is still 2.41 Å. This result can also be confirmed by **Figure 2B** where H_2CO is almost surrounded by cyan, and only 0.01 e was obtained from the original monolayer MoS_2. In order to further understand the interaction between the adsorbed H_2CO and the original monolayer MoS_2, we also calculated the TDOS of S/H_2CO structure and the DOS of H_2CO before and after adsorption, as shown in **Figure 2C**. After the adsorption of H_2CO, we can see that there is no induced impurity state, and the band gap has no obvious change. Just because of the introduction of molecules, the single peak increases, indicating that the adsorption almost does not change the electrical properties of the original monolayer MoS_2, It is well consistent with the literature report (Ma et al., 2016b). In other words, the original monolayer MoS_2 is not sensitive to H_2CO, which further proves that the adsorption of H_2CO on the original monolayer MoS_2 belongs to physical adsorption.

Adsorption of H_2CO on Zn Doped Monolayer MoS_2 (Zn/H_2CO)

Finally, four stable configurations of H_2CO adsorption structure on Zn-MoS_2 were obtained, including Zn/H_2CO-(a), Zn/H_2CO-(b), Zn/H_2CO-(c) and Zn/H_2CO-(d). The structure parameters are shown in **Figure 3**, and the other related parameters are shown in **Table 1**.

Configuration of the Adsorbed Zn/H_2CO-(a) and Zn/H_2CO-(b)

As shown in **Figure 3A,B**, the adsorption energies of Zn/H_2CO-(a) and Zn/H_2CO-(b) are 0.98 and 0.80 eV, respectively. The distance between the O atoms of the adsorbed molecule and Zn dopant is 1.98 and 1.95 Å, respectively, indicating that the

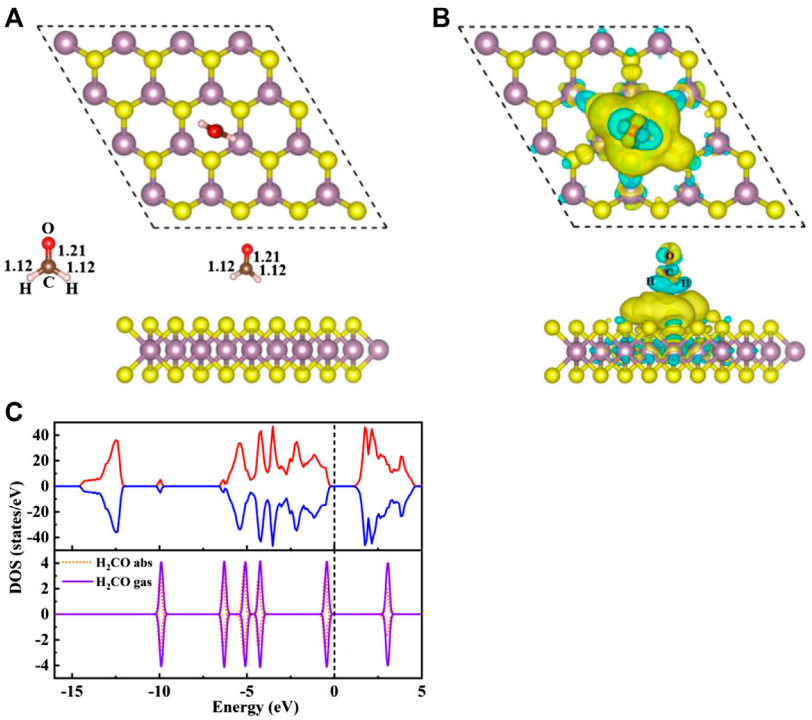

FIGURE 2 | (A) The top view **(top)** and side view **(bottom)** structure of S/H_2CO, and the left side shows the structure of H_2CO in the gas phase. **(B)** Charge density difference diagram of S/H_2CO. The yellow area indicates charge accumulation and the cyan area indicates charge loss. **(C)** The spin polarized TDOS of S/H_2CO **(upper panels)** and the projected density of states (PDOS) of the original monolayer MoS_2 for H_2CO adsorption **(lower panels)**: Orange dotted line, H_2CO in the adsorption state; purple curve, H_2CO in the gas phase. The positive and negative values of DOS indicate spin up and spin down, respectively. The Fermi level is marked with a black dotted line.

molecule has strong adsorbed ability. The interaction between the adsorbed H_2CO and the substrate makes the geometry of H_2CO change obviously, the C-O bond length of H_2CO increased by 0.04 Å and the C-H bond length decreased by 0.02 Å. The average bond length of Zn-Mo on the substrate Zn-MoS_2 increases from 2.41 to 2.70 Å, and the distance between the dopant Zn and the S-plane is 0.33 and 0.28 Å larger than that of the substrate Zn-MoS_2, respectively. In addition, Bader charge analysis showed that H_2CO was the electron acceptor of Zn/H_2CO-(a) and Zn/H_2CO-(b), and the electron transfer between Zn-MoS_2 substrate and H_2CO was 0.05 and 0.09 *e*, respectively, this is mainly due to the doping of Zn atoms (0.51 and 0.53 *e*), it may be due to the difference of electronegativity between O (3.44) and Zn (1.65).

The difference of charge density of the final configuration of Zn/H_2CO-(a) and Zn/H_2CO-(b) is shown in **Figures 4A,B** to further understand the interaction between H_2CO molecule and Zn doped monolayer MoS_2. The yellow area is the electron accumulation area, and the cyan area is the electron consumption area. As shown in **Figure 4A**, the electron transfer is not only located on the C and O atoms of H_2CO adsorption, but also on the O-Zn bond, which is consistent with the strong adsorption capacity of H_2CO. In addition, the loss of electrons on the C-O bond leads to the weakening of the C-O bond, which makes the O atom protruding above the S plane chemically active to other molecules, including H_2CO itself. For the adsorption of Zn/H_2CO-(b), it can be found that the adsorption behavior is similar to that of Zn/H_2CO-(a), as shown in **Figure 4B**, which will not be further discussed.

In order to further understand the adsorption behavior of H_2CO on Zn-MoS_2 surface. **Figures 5A–D** displayed the spin-polarized total densities of states (TDOS) (upper panels) and corresponding DOS projected on 3*d* states of Zn atom, adsorbed H_2CO gas molecules and the isolated H_2CO gas molecules (lower panels) after H_2CO adsorption on Zn-embedded monolayer MoS_2.

The TDOS of Zn/H_2CO-(a) and Zn/H_2CO-(b) systems are shown in **Figures 5A,B**. Compared with Zn-MoS_2, due to the hybridization of Zn atoms and H_2CO molecules, the charge is transferred from the matrix to the adsorbed H_2CO molecule, resulting in a new DOS peak at CBM for the TDOS of Zn/H_2CO-(a) and Zn/H_2CO-(b) systems. It can be observed that the occupied state PDOS of the adsorbed H_2CO molecule **Figures 5A,B**, below is much lower panels than Fermi level, and the induced impurity state is produced, which reveals the reaction between Zn-MoS_2 monolayer and H_2CO molecule. For Zn/H_2CO-(a) and Zn/H_2CO-(b) configurations, the molecular orbitals of adsorbed H_2CO are delocalized relative to the isolated H_2CO in the gas phase. The 3*d* orbital of Zn atom is coupled with H_2CO in the range of 9.60~0.00 eV. The interaction between H_2CO molecule and Zn atom leads to charge transfer. Zn/H_2CO-(a) and Zn/H_2CO-(b) structures have higher adsorption energy, which indicates that the adsorption is

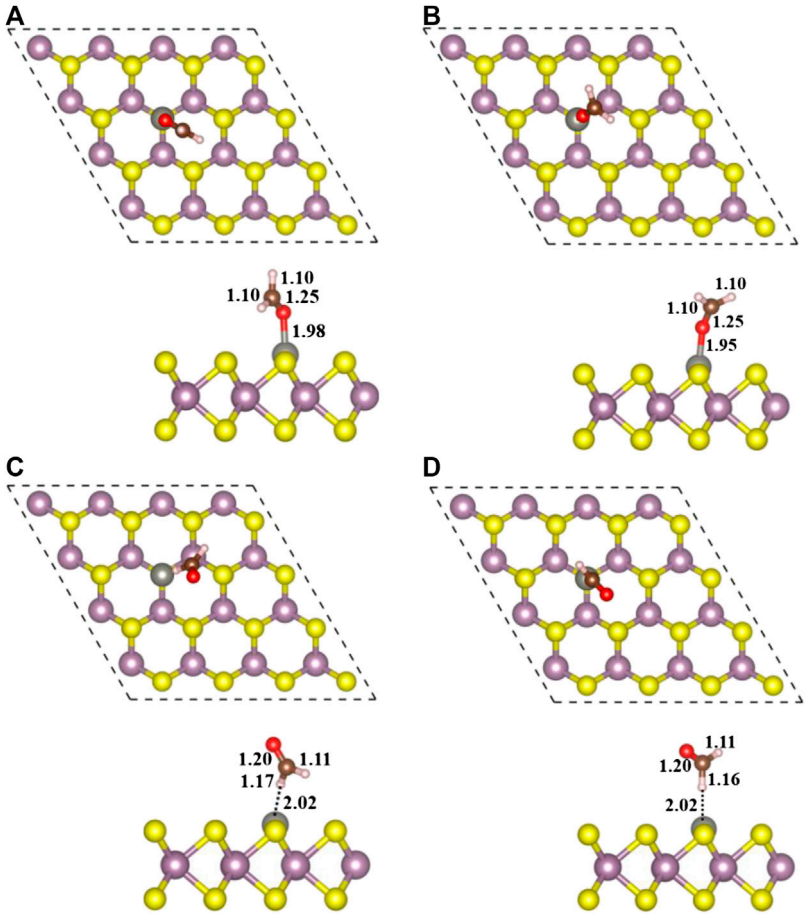

FIGURE 3 | Top view **(top)** and side view **(bottom)** of geometric structures of Zn/H_2CO-**(A)**, Zn/H_2CO-**(B)**, Zn/H_2CO-**(C)** and Zn/H_2CO-**(D)** configurations are shown in **(A–D)**, respectively.

chemisorption, which is suitable for gas removal under H_2CO adsorption. The results show that, compared with undoped MoS_2, doping Zn atoms in the defective monolayer MoS_2 is beneficial to the adsorption of H_2CO. We use crystal orbital Hamiltonian populations (COHP) to analyze the interaction between different O-Zn/H-Zn bonds by means of a pair of atomic orbital bonding or antibonding states (van Santen and Tranca, 2016; Steinberg and Dronskowski, 2018; Tsuji and Yoshizawa, 2018). Moreover, through the integration of COHP (ICOHP), we can get a precise value of bond strength. The positive and negative values of ICOHP represent the anti bonding state and bonding state respectively. The smaller the ICOHP value, the stronger the bond strength. **Figures 6A-D** shows the -COHP curve and the integral (ICOHP) value of the O-Zn and H-Zn bonds in the structured Zn/H_2CO-(a) and Zn/H_2CO-(b) systems and the Zn/H_2CO-(c) and Zn/H_2CO-(d) systems, respectively. It can be seen from **Figures 6A,B** that when H_2CO is adsorbed to Zn-MoS_2, there are a small amount of O-Zn bonding orbitals (-COHP values) at Fermi level, and the orbitals above Fermi level belong to anti bonding orbitals. In other words, the O-Zn bond is enhanced after H_2CO adsorption, which is consistent with the increase of C-O distance (**Figures 4A,B**). The O atoms in the two adsorption systems have strong binding with Zn atoms (ICOHP value is small), which also shows that these phases are stable.

Configuration Adsorption of Zn/H_2CO-(c) and Zn/H_2CO-(d)

As shown in **Figures 3C,D** the Zn/H_2CO-(c) and Zn/H_2CO-(d) configurations with adsorption energies of 0.15 and 0.11 eV, respectively, are much less stable than those of Zn/H_2CO-(a) and Zn/H_2CO-(b), and the H atoms point to the doped Zn atoms. Different from the configurations of Zn/H_2CO-(a) and Zn/H_2CO-(b), the adsorption energies are also very different, similar to the adsorption on the original monolayer MoS_2. Therefore, the orientation of H atom or O atom in H_2CO can be used to determine the adsorption energy. At the same time, in **Figures 3C,D** the interaction between the adsorbed molecules and the substrate is also different due to the different orientations of hydrogen atoms, i.e., the angle of C-H-Zn is different. In the two structures, the distance between H and Zn atoms is 2.02 Å.

Therefore, the strong covalent bond or ionic bond between the two atoms can be eliminated. The weak electrostatic attraction of negatively charged H atom (0.06 *e*) and positively charged Zn atom

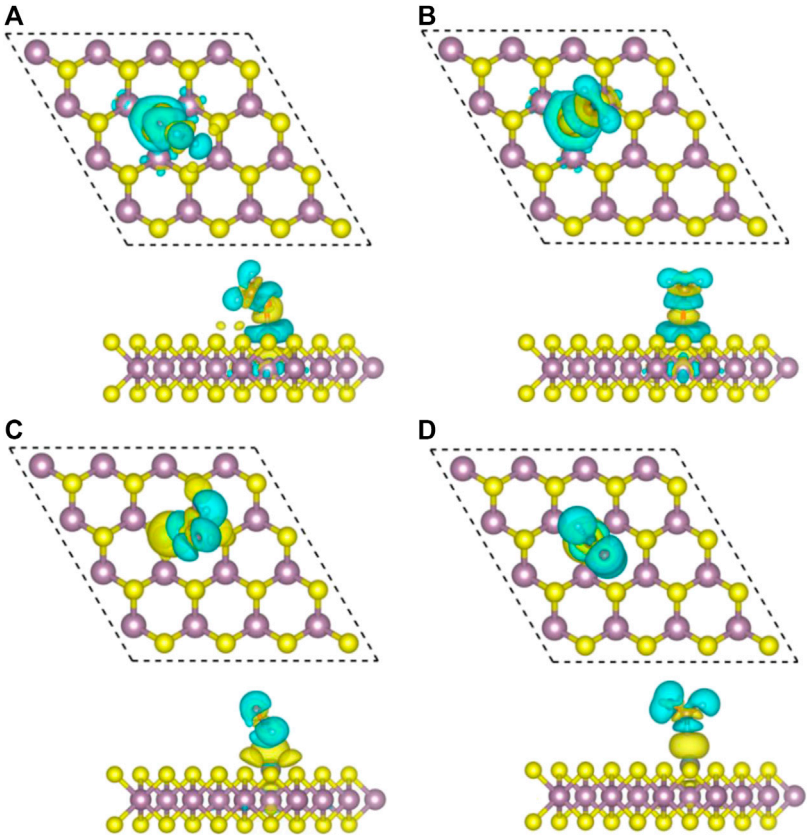

FIGURE 4 | Top view **(top)** and side view **(bottom)** of charge density differences of final configurations of Zn/H_2CO-**(A)**, Zn/H_2CO-**(B)**, Zn/H_2CO-**(C)** and Zn/H_2CO-**(D)** are shown in **(A–D)**, respectively. Yellow and cyan represent regions of electron accumulation and depletion, respectively.

(0.33 *e*) should be combined, which is consistent with the weak adsorption of Zn/H_2CO-(c) and Zn/H_2CO-(d) configurations.

Compared with H_2CO in the gas phase, the geometry and substrate of the adsorbed state are only slightly changed. The C-O bond of H_2CO decreased by 0.01 Å. In addition, for Zn/H_2CO-(c) and Zn/H_2CO-(d), there is a small electron transfer (0.07 and 0.08 *e*) between the adsorbed H_2CO and the substrate, and the molecule has a small magnetic moment of 0.01 μ_B. The adsorption of Zn/H_2CO-(c) and Zn/H_2CO-(d) is weaker than that of Zn/H_2CO-(a) and Zn/H_2CO-(b), indicating that the probability of occurrence of the latter two configurations is much higher than that of the former two. For the adsorption of Zn/H_2CO-(c) and Zn/H_2CO-(d) configurations, the charge density difference diagram shows that there is almost no electron accumulation between the adsorbed molecule H_2CO and the Zn doped MoS_2 monolayer (**Figures 4C,D**). It is further confirmed that the adsorption capacity of H_2CO on the substrate is weak, which is consistent with the small adsorption energy and large distance mentioned above.

Further analyzing the adsorption behavior of H_2CO on the Zn-MoS_2 surface, it can be seen from **Figures 5C,D** above that the TDOS of the Zn/H_2CO-(c) and Zn/H_2CO-(d) systems do not show induced impurity state near the Fermi level, and the DOS curves of the adsorbed H_2CO of the Zn/H_2CO-(c) and Zn/H_2CO-(d) systems overlap slightly with the 3*d* orbitals of the Zn atoms (**Figures 5C,D**, below), shows that the interaction between H_2CO and Zn-MoS_2 is weak, the bonding between H-Zn atoms is weak, and the ICOHP negative value is large (**Figures 6C,D**), resulting in only 0.07 and 0.08 *e* being transferred from the adsorbed H_2CO molecule to the final substance. The H-Zn strength in Zn/H_2CO-(c) system is higher than that in Zn/H_2CO-(d) system, indicating that Zn/H_2CO-(c) system is more stable than Zn/H_2CO-(d) system. This conclusion is consistent with the previous calculation of adsorption energy (**Table 1**). In terms of magnetic properties, the total magnetic moment of the whole adsorption system did not change after adsorption of H_2CO by Zn-MoS_2 (Zn/H_2CO-(c) and Zn/H_2CO-(d) were 2.00 μ_B), which was consistent with the small adsorption energy of Zn/H_2CO-(c) and Zn/H_2CO-(d).

CONCLUSION

In conclusion, according to the first principles calculations, we have studied the effects of Zn doping S vacancy on the electronic structure, magnetic properties and chemical activity of monolayer MoS_2. The calculation of binding energy shows that Zn atoms are closely bound to S-defects, which is mainly due to the hybridization between dopant atoms and their nearest Mo

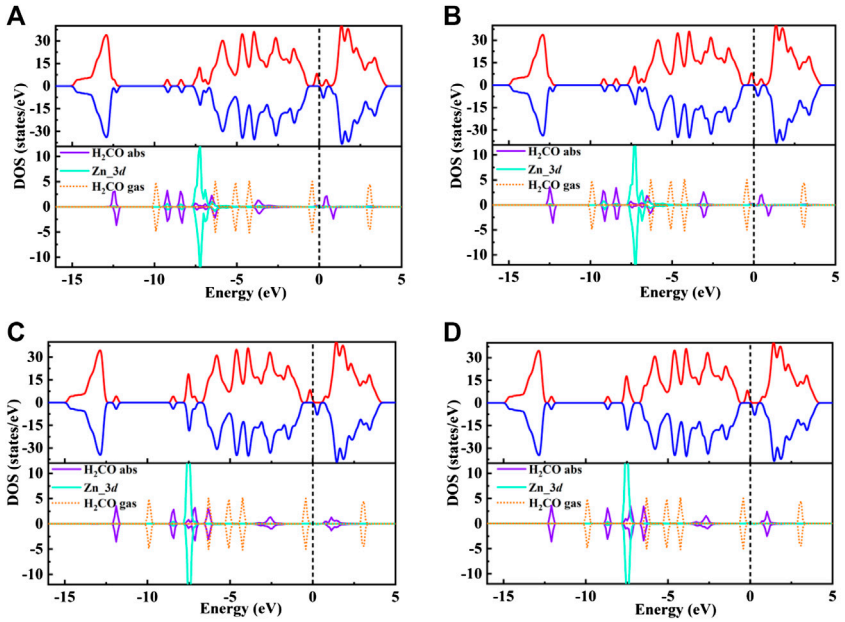

FIGURE 5 | (A–D) shows the total spin polarized density of states (TDOS) of Zn/H_2CO-**(A)**, Zn/H_2CO-**(B)**, Zn/H_2CO-**(C)** and Zn/H_2CO-**(D)** systems **(upper panels)**, and the projected density of states (PDOS) of H_2CO adsorbed by Zn-MoS_2 **(lower panels)**: Purple curve, H_2CO in adsorption state; orange dotted line, H_2CO in gas phase; blue curve, *d*-projected PDOS for Zn atom. The positive and negative values of DOS indicate spin up and spin down, respectively. The Fermi level is marked with a black dotted line.

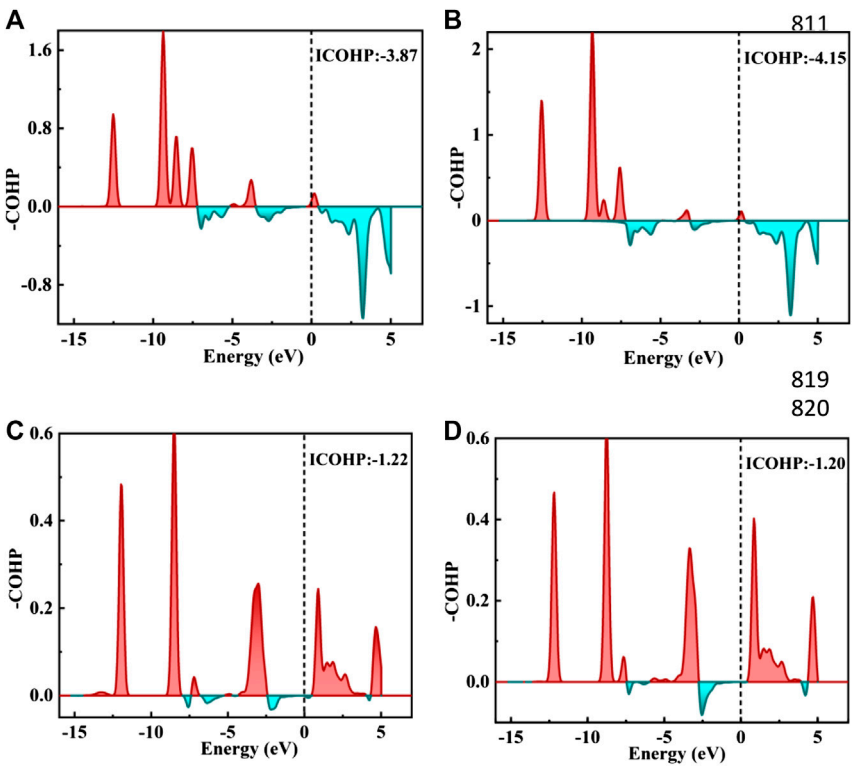

FIGURE 6 | (A–D) figure shows the negative crystal orbital Hamilton density (-COHP) on the Zn/H_2CO-**(A)** and Zn/H_2CO-**(B)** system O-Zn bond and the Zn/H_2CO-**(C)** and Zn/H_2CO-**(D)** system H-Zn bond, respectively. The red filled area is the O-Zn/H-Zn bonding area, and the green filled area is the O-Zn/H-Zn antibonding. Fermi energy level marked with black dotted line.

atoms. Finally, a new single cluster catalyst on $ZnMo_3$ surface is formed, which improves the selectivity of MoS_2 surface. By embedding Zn atoms, the magnetic properties of MoS_2 monolayer can be adjusted and the spin magnetic moment of Zn-MoS_2 is 2.00 μ_B. The electronic properties of MoS_2 are also changed by the impurity states induced in the band gap. The effects of H_2CO adsorption and doping on the chemical activity of MoS_2 monolayers were further investigated. It was found that the H-end downward adsorption of H_2CO in the original monolayer MoS_2 and Zn doped monolayer MoS_2 was very weak, and the electronic structure of the two substrates changed little after adsorption, indicating that the two systems were not sensitive to H_2CO.When the O atom in H_2CO molecule faces to the substrate, the adsorption capacity is strong, and the adsorbed H_2CO is effectively activated. DOS analysis showed that the electronic structure of Zn-MoS_2 could be changed by introducing impurities in the band gap when the O-terminal of H_2CO molecule was adsorbed downward. At the same time, the magnetic properties of Zn-MoS_2 system are also adjusted. The COHP diagram shows that Zn atoms are strongly bonded with O atoms. This study shows that Zn doping is a promising method to optimize the electronic structure, magnetic properties and chemical activity of MoS_2, which provides a promising way to improve the electronic properties of MoS_2 materials.

AUTHOR CONTRIBUTIONS

CH: conceptualization, methodology, funding acquisition, supervision, project administration. GZ: formal analysis. JH: software. TX: software, methodology. HL: writing—original draft, investigation, formal analysis, methodology. LF: supervision, funding acquisition, project administration. GD: formal analysis. HY: software.

DATA AVAILABILITY STATEMENT

The original contributions presented in the study are included in the article/**Supplementary Material**, further inquiries can be directed to the corresponding authors.

FUNDING

This study was funded by the Natural Science Foundation of China (Nos. 21603109 and 21876104), the Henan Joint Fund of the National Natural Science Foundation of China (No. U1404216), Transformation of Scientific and Technological Achievements Programs of Higher Education Institutions in Shanxi (No. 2020CG032), Cultivation Plan of Young Scientific Researchers in Higher Education Institutions of Shanxi Province.

SUPPLEMENTARY MATERIAL

The Supplementary Material for this article can be found online at: https://www.frontiersin.org/articles/10.3389/fchem.2020.605311/full#supplementary-material.

REFERENCES

Abbas, H. G., Debela, T. T., Hussain, S., and Hussain, I. (2018). Inorganic molecule (O_2, NO) adsorption on nitrogen- and phosphorus-doped MoS_2 monolayer using first principle calculations. *RSC Adv.* 8 (67), 38656–38666. doi:10.1039/c8ra07638c

Abbasi, A. (2019). Adsorption of phenol, hydrazine and thiophene on stanene monolayers: a computational investigation. *Synth. Met.* 247, 26–36. doi:10.1016/j.synthmet.2018.11.012

Abbasi, A., and Sardroodi, J. J. (2018a). Exploration of sensing of nitrogen dioxide and ozone molecules using novel TiO_2/Stanene heterostructures employing DFT calculations. *Appl. Surf. Sci.* 442, 368–381. doi:10.1016/j.apsusc.2018.02.183

Abbasi, A., and Sardroodi, J. J. (2018b). Investigation of the adsorption of ozone molecules on TiO_2/WSe_2 nanocomposites by DFT computations: applications to gas sensor devices. *Appl. Surf. Sci.* 436, 27–41. doi:10.1016/j.apsusc.2017.12.010

Abbasi, A., and Sardroodi, J. J. (2019). The adsorption of sulfur trioxide and ozone molecules on stanene nanosheets investigated by DFT: applications to gas sensor devices. *Phys. E Low-Dimens. Syst. Nanostruct.* 108, 382–390. doi:10.1016/j.physe.2018.05.004

Allred, A. L. (1961). Electronegativity values from thermochemical data. *J. Inorg. Nucl. Chem.* 17 (3-4), 215–221. doi:10.1016/0022-1902-5

Ataca, C., and Ciraci, S. (2011). Functionalization of single-layer MoS_2 honeycomb structures. *J. Phys. Chem. C* 115 (27), 13303–13311. doi:10.1021/jp2000442

Chen, D., Tang, J., Zhang, X., Li, Y., and Liu, H. (2019). Detecting decompositions of sulfur hexafluoride using MoS_2 monolayer as gas sensor. *IEEE Sensor. J.* 19 (1), 39–46. doi:10.1109/jsen.2018.2876637

Chung, P. R., Tzeng, C. T., Ke, M. T., and Lee, C. Y. (2013). Formaldehyde gas sensors: a review. *Sensors.* 13 (4), 4468–4484. doi:10.3390/s130404468

Cui, H., Zhang, X., Zhang, G., and Tang, J. (2019). Pd-doped MoS_2 monolayer: a promising candidate for DGA in transformer oil based on DFT method. *Appl. Surf. Sci.* 470, 1035–1042. doi:10.1016/j.apsusc.2018.11.230

DimpleJena, N., and De Sarkar, A. (2017). Compressive strain induced enhancement in thermoelectric-power-factor in monolayer MoS_2 nanosheet. *J. Phys. Condens. Matter.* 29 (22), 225501. doi:10.1088/1361-648X/aa6cbc

Guo, J., Tadesse Tsega, T., Ul Islam, I., Iqbal, A., Zai, J., and Qian, X. (2020). Fe doping promoted electrocatalytic N_2 reduction reaction of 2H MoS_2. *Chin. Chem. Lett.* 31(09): 2487–2490. doi:10.1016/j.cclet.2020.02.019

Guo, T., Wang, L., Sun, S., Wang, Y., Chen, X., Zhang, K., et al. (2019). Layered MoS_2@graphene functionalized with nitrogen-doped graphene quantum dots as an enhanced electrochemical hydrogen evolution catalyst. *Chin. Chem. Lett.* 30 (6), 1253–1260. doi:10.1016/j.cclet.2019.02.009

Henkelman, G., Arnaldsson, A., and Jónsson, H. (2006). A fast and robust algorithm for Bader decomposition of charge density. *Comput. Mater. Sci.* 36 (3), 354–360. doi:10.1016/j.commatsci.2005.04.010

Kathiravan, D., Huang, B.-R., Saravanan, A., Prasannan, A., and Hong, P.-D. (2019). Highly enhanced hydrogen sensing properties of sericin-induced exfoliated MoS_2 nanosheets at room temperature. *Sensor. Actuator. B Chem.* 279, 138–147. doi:10.1016/j.snb.2018.09.104

Kwak, I. H., Kwon, I. S., Abbas, H. G., Jung, G., Lee, Y., Park, J., et al. (2018). Stable methylammonium-intercalated 1T′-MoS_2 for efficient electrocatalytic hydrogen evolution. *J. Mater. Chem.* 6 (14), 5613–5617. doi:10.1039/c8ta00700d

Kwon, I. S., Kwak, I. H., Abbas, H. G., Jung, G., Lee, Y., Park, J., et al. (2018). Intercalation of aromatic amine for the 2H-1T′ phase transition of MoS_2 by experiments and calculations. *Nanoscale* 10 (24), 11349–11356. doi:10.1039/c8nr02365d

Lara-Ibeas, I., Megías-Sayago, C., Louis, B., and Le Calvé, S. (2020). Adsorptive removal of gaseous formaldehyde at realistic concentrations. *J. Environ. Chem. Eng.* 8 (4), 103986. doi:10.1016/j.jece.2020.1

Le, D., Rawal, T. B., and Rahman, T. S. (2014). Single-layer MoS_2 with sulfur vacancies: structure and catalytic application. *J. Phys. Chem. C* 118 (10), 5346–5351. doi:10.1021/jp411256g

Lolla, S., and Luo, X. (2020). Tuning the catalytic properties of monolayer MoS2 through doping and sulfur vacancies. *Appl. Surf. Sci.* 507, 144892. doi:10.1016/j.apsusc.2019.144892

Luo, H., Cao, Y., Zhou, J., Feng, J., Cao, J., and Guo, H. (2016). Adsorption of NO_2, NH_3 on monolayer MoS_2 doped with Al, Si, and P: a first-principles study. *Chem. Phys. Lett.* 643, 27–33. doi:10.1016/j.cplett.2015.10.077

Ma, D., Ju, W., Li, T., Yang, G., He, C., Ma, B., et al. (2016a). Formaldehyde molecule adsorption on the doped monolayer MoS_2: a first-principles study. *Appl. Surf. Sci.* 371, 180–188. doi:10.1016/j.apsusc.2016.02.230

Ma, D., Ju, W., Li, T., Zhang, X., He, C., Ma, B., et al. (2016b). The adsorption of CO and NO on the MoS_2 monolayer doped with Au, Pt, Pd, or Ni: a first-principles study. *Appl. Surf. Sci.* 383, 98–105. doi:10.1016/j.apsusc.2016.04.171

Ma, D., Wang, Q., Li, T., He, C., Ma, B., Tang, Y., et al. (2016c). Repairing sulfur vacancies in the MoS_2 monolayer by using CO, NO and NO_2 molecules. *J. Mater. Chem. C* 4 (29), 7093–7101. doi:10.1039/c6tc01746k

Ma, X. L., Liu, J. C., Xiao, H., and Li, J. (2018). Surface single-cluster catalyst for N_2-to-NH_3 thermal conversion. *J. Am. Chem. Soc.* 140 (1), 46–49. doi:10.1021/jacs.7b10354

Maintz, S., Deringer, V. L., Tchougreeff, A. L., and Dronskowski, R. (2016). LOBSTER: a tool to extract chemical bonding from plane-wave based DFT. *J. Comput. Chem.* 37 (11), 1030–1035. doi:10.1002/jcc.24300

Momma, K., and Izumi, F. (2011). VESTA 3 for three-dimensional visualization of crystal, volumetric and morphology data. *J. Appl. Crystallogr.* 44 (6), 1272–1276. doi:10.1107/s0021889811038970

Monkhorst, H. J., and Pack, J. D. (1976). Special points for Brillouin-zone integrations. *Phys. Rev. B* 13 (12), 5188–5192. doi:10.1103/PhysRevB.13.5188

Pan, X., Ji, J., Zhang, N., and Xing, M. (2020). Research progress of graphene-based nanomaterials for the environmental remediation. *Chin. Chem. Lett.* 31 (6), 1462–1473. doi:10.1016/j.cclet.2019.10.002

Qian, G., Peng, Q., Zou, D., Wang, S., Yan, B., and Zhou, Q. (2020). First-principles insight into Au-doped MoS_2 for sensing C_2H_6 and C_2H_4. *Front. Mater.* 7. doi:10.3389/fmats.2020.00022

Qian, H., Lu, W., Wei, X., Chen, W., and Deng, J. (2019). H_2S and SO_2 adsorption onPt-MoS_2 adsorbent for partial discharge elimination: a DFT study. *Results Phys.* 12, 107–112. doi:10.1016/j.rinp.2018.11.035

Ren, J., Liu, H., Xue, Y., and Wang, L. (2019). Adsorption behavior of CH_4 gas molecule on the MoX_2(S, Se, Te) monolayer: the DFT study. *Nanoscale Res. Lett.* 14 (1), 293. doi:10.1186/s11671-019-3125-5

Sahoo, M. P. K., Wang, J., Zhang, Y., Shimada, T., and Kitamura, T. (2016). Modulation of gas adsorption and magnetic properties of monolayer-MoS2 by antisite defect and strain. *J. Phys. Chem. C* 120 (26), 14113–14121. doi:10.1021/acs.jpcc.6b03284

Salthammer, T. (2013). Formaldehyde in the ambient atmosphere: from an indoor pollutant to an outdoor pollutant? *Angew. Chem. Int. Ed.* 52 (12), 3320–3327. doi:10.1002/anie.201205984

Sharma, A., AnuKhan, M. S., Husain, M., Khan, M. S., and Srivastava, A. (2018). Sensing of CO and NO on Cu-doped MoS_2 monolayer-based single electron transistor: a first principles study. *IEEE Sensor. J.* 18 (7), 2853–2860. doi:10.1109/jsen.2018.2801865

Song, X., Dong, M., Li, Y., Wu, Y., Sun, Y., Yuan, G., et al. (2020). Formaldehyde adsorption effects of chlorine adatoms on lithium-decorated graphene: a DFT study. *Chem. Phys. Lett.* 761, 138085. doi:10.1016/j.cplett.2020.1380

Steinberg, S., and Dronskowski, R. (2018). The crystal orbital Hamilton population (COHP) method as a tool to visualize and analyze chemical bonding in intermetallic compounds. *Crystals.* 8 (5), 225. doi:10.3390/cryst8050225

Tan, J., Hu, J., Ren, J., Peng, J., Liu, C., Song, Y., et al. (2020). Fast response speed of mechanically exfoliated MoS_2 modified by PbS in detecting NO_2. *Chin. Chem. Lett.* 31 (8), 2103–2108. doi:10.1016/j.cclet.2020.03.060

Tsuji, Y., and Yoshizawa, K. (2018). Adsorption and activation of methane on the (110) surface of rutile-type metal dioxides. *J. Phys. Chem. C* 122 (27), 15359–15381. doi:10.1021/acs.jpcc.8b03184

van Santen, R. A., and Tranca, I. (2016). How molecular is the chemisorptive bond? *Phys. Chem. Chem. Phys.* 18 (31), 20868–20894. doi:10.1039/c6cp01394e

Wang, J., Zhou, Q., Lu, Z., Wei, Z., and Zeng, W. (2019a). Gas sensing performances and mechanism at atomic level of Au-MoS_2 microspheres. *Appl. Surf. Sci.* 490, 124–136. doi:10.1016/j.apsusc.2019.06.075

Wang, J., Zhou, Q., and Zeng, W. (2019b). Competitive adsorption of SF_6 decompositions on Ni-doped ZnO (100) surface: computational and experimental study. *Appl. Surf. Sci.* 479, 185–197. doi:10.1016/j.apsusc.2019.01.255

Wang, T., Gao, D., Zhuo, J., Zhu, Z., Papakonstantinou, P., Li, Y., et al. (2013). Size-dependent enhancement of electrocatalytic oxygen-reduction and hydrogen-evolution performance of MoS_2 particles. *Chemistry* 19 (36), 11939–11948. doi:10.1002/chem.201301406

Wanno, B., and Tabtimsai, C. (2014). A DFT investigation of CO adsorption on VIIIB transition metal- doped graphene sheets. *Superlattice. Microst.* 67, 110–117. doi:10.1016/j.spmi.2013.12.025

Wu, D., Lou, Z., Wang, Y., Yao, Z., Xu, T., Shi, Z., et al. (2018). Photovoltaic high-performance broadband photodetector based on MoS_2/Si nanowire array heterojunction. *Sol. Energy Mater. Sol. Cell.* 182, 272–280. doi:10.1016/j.solmat.2018.03.017

Xu, M., Liang, T., Shi, M., and Chen, H. (2013). Graphene-like two-dimensional materials. *Chem. Rev.* 113 (5), 3766–3798. doi:10.1021/cr300263a

Yu, L., El-Damak, D., Radhakrishna, U., Ling, X., Zubair, A., Lin, Y., et al. (2016). Design, modeling, and fabrication of chemical vapor deposition grown MoS_2 circuits with E-mode FETs for large-area electronics. *Nano Lett.* 16 (10), 6349–6356. doi:10.1021/acs.nanolett.6b02739

Zhang, D., Jiang, C., and Wu, J. (2018). Layer-by-layer assembled In_2O_3 nanocubes/flower-like MoS_2 nanofilm for room temperature formaldehyde sensing. *Sensor. Actuator. B Chem.* 273, 176–184. doi:10.1016/j.snb

Zhang, D., Sun, Y. E., Jiang, C., and Zhang, Y. (2017). Room temperature hydrogen gas sensor based on palladium decorated tin oxide/molybdenum disulfide ternary hybrid via hydrothermal route. *Sensor. Actuator. B Chem.* 242, 15–24. doi:10.1016/j.snb.2016.11.005

Zhang, Y., Zeng, W., and Li, Y. (2019). Porous MoS_2 microspheres decorated with Cu_2O nanoparticles for ammonia sensing property. *Mater. Lett.* 241, 223–226. doi:10.1016/j.matlet.2019.01.130

Zheng, J., Song, D., Chen, H., Xu, J., Alharbi, N. S., Hayat, T., et al. (2020). Enhanced peroxidase-like activity of hierarchical MoS_2-decorated N-doped carbon nanotubes with synergetic effect for colorimetric detection of H_2O_2 and ascorbic acid. *Chin. Chem. Lett.* 31 (5), 1109–1113. doi:10.1016/j.cclet.2019.09.037

Zhou, J., Liu, G., Jiang, Q., Zhao, W., Ao, Z., and An, T. (2020). Density functional theory calculations on single atomic catalysis: Ti-decorated $Ti_3C_2O_2$ monolayer (MXene) for HCHO oxidation. *Chin. J. Catal.* 41 (10), 1633–1644. doi:10.1016/s1872-2067(20)63571-9

Zhou, Q., Hong, C., Yao, Y., Hussain, S., Xu, L., Zhang, Q., et al. (2018). Hierarchically MoS_2 nanospheres assembled from nanosheets for superior CO gas-sensing properties. *Mater. Res. Bull.* 101, 132–139. doi:10.1016/j.materresbull.2018.01.030

Conflict of Interest: The authors declare that the research was conducted in the absence of any commercial or financial relationships that could be construed as a potential conflict of interest.